

Variation of structural, electrical, and optical properties of Zn 1 – x Mg x O thin films

Jae Won Kim, Hong Seong Kang, Jong Hoon Kim, Sang Yeol Lee, Jung-Kun Lee, and Michael Nastasi

Citation: *Journal of Applied Physics* **100**, 033701 (2006); doi: 10.1063/1.2219153

View online: <http://dx.doi.org/10.1063/1.2219153>

View Table of Contents: <http://scitation.aip.org/content/aip/journal/jap/100/3?ver=pdfcov>

Published by the [AIP Publishing](http://www.aip.org)

Articles you may be interested in

Structural, optical, and electrical properties of Yb-doped ZnO thin films prepared by spray pyrolysis method
J. Appl. Phys. **109**, 033708 (2011); 10.1063/1.3544307

Structural, electrical, and optical characterizations of epitaxial Zn 1 – x Ga x O films grown on sapphire (0001) substrate
J. Appl. Phys. **101**, 124912 (2007); 10.1063/1.2749487

Effect of thickness on structural, electrical, and optical properties of ZnO: Al films deposited by pulsed laser deposition
J. Appl. Phys. **101**, 033713 (2007); 10.1063/1.2437572

Structural and optical properties of Zn 1 – x Mg x O nanocrystals obtained by low temperature method
J. Appl. Phys. **100**, 034315 (2006); 10.1063/1.2227708

Blueshift of near band edge emission in Mg doped ZnO thin films and aging
J. Appl. Phys. **95**, 4772 (2004); 10.1063/1.1690091

The advertisement features a dark blue background with a film strip on the left side. The film strip shows a purple and yellow textured surface. The text is centered and right-aligned. The main headline is 'Not all AFMs are created equal' in orange. Below it, 'Asylum Research Cypher™ AFMs' is written in white. The tagline 'There's no other AFM like Cypher' is in orange. At the bottom left, the website 'www.AsylumResearch.com/NoOtherAFMLikeIt' is in white. At the bottom right, the Oxford Instruments logo is shown, consisting of the word 'OXFORD' in a white box above 'INSTRUMENTS' in a smaller white box, with the tagline 'The Business of Science®' below it.

Not all AFMs are created equal
Asylum Research Cypher™ AFMs
There's no other AFM like Cypher

www.AsylumResearch.com/NoOtherAFMLikeIt

OXFORD
INSTRUMENTS
The Business of Science®

Variation of structural, electrical, and optical properties of Zn_{1-x}Mg_xO thin films

Jae Won Kim, Hong Seong Kang, Jong Hoon Kim, and Sang Yeol Lee^{a)}

Department of Electrical and Electronic Engineering, Yonsei University, 134 Shinchon-dong, Seodaemun-ku, Seoul, Korea 120-749

Jung-Kun Lee and Michael Nastasi

Materials Science and Technology Division, Los Alamos National Laboratory, Los Alamos, New Mexico 87545

(Received 18 July 2005; accepted 31 May 2006; published online 1 August 2006)

Zn_{1-x}Mg_xO thin films on (001) sapphire substrates were deposited using pulsed laser deposition. As the substrate temperature increased, the Mg content in the Zn_{1-x}Mg_xO thin films increased and the photoluminescence (PL) peak position of the Zn_{1-x}Mg_xO thin films shifted from 370 to 356 nm, indicating a band gap expansion. Variations of the structural, electrical, and optical properties of Zn_{1-x}Mg_xO thin films have been observed and analyzed by x-ray diffraction, Hall measurements, and PL measurements. © 2006 American Institute of Physics. [DOI: 10.1063/1.2219153]

I. INTRODUCTION

ZnO is an appealing material for optoelectronic devices, such as light emitting diodes (LEDs) and laser diodes (LDs), due to its wide band gap of 3.37 eV at room temperature and a large exciton binding energy of 60 meV.¹ For ZnO-based *p-n* junction devices, the fabrication of *p*-type ZnO devices and band gap modulation are important. Zn_{1-x}Mg_xO alloy used as a barrier layer for the band gap modulation and ZnO/(Mg,Zn)O multiple quantum wells grown on a lattice-matched ScAlMgO₄ substrate have been reported.^{2,4-6}

Recently, a Zn_{1-x}Mg_xO thin film has been deposited using various deposition techniques, such as laser molecular beam epitaxy (LMBE),² metalorganic vapor-phase epitaxy (MOVPE),³ rf magnetron sputtering,⁴ sol-gel deposition,⁵ and pulsed laser deposition (PLD).^{6,7} Particularly, the PLD has advantages because it employs a relatively high oxygen partial pressure and achieves high quality films with a relatively high deposition rate at a low temperature due to the ablated particles of high energy (~100 eV) obtained in the laser-produced plume.⁸

An alloy of ZnO and MgO is expected easily because the ionic radius of Mg²⁺ (0.57 Å) is similar to that of Zn²⁺ (0.60 Å). According to the phase diagram of the ZnO–MgO binary system, the thermodynamic solid solubility of MgO in ZnO is less than 4 mol %. However, it has been reported that the solid solubility of MgO in ZnO is greater than 33 mol % for thin film alloys grown under metastable conditions.³⁻⁶ Zn-related species can be easily desorbed at higher growth temperatures since Zn-related species have a higher vapor pressure than that of Mg.⁷ However, there has been no systematic study of the effect of the deposition temperature and postannealing on the properties of the wurtzite-phase Zn_{1-x}Mg_xO thin films deposited using PLD.

In this study, the variation of the optical, structural, and

electrical properties of Zn_{1-x}Mg_xO thin films has been systematically investigated according to substrate temperature variations and postannealing.

II. EXPERIMENT

Zn_{1-x}Mg_xO thin films were deposited by PLD on (001) sapphire substrates using a Zn_{0.7}Mg_{0.3}O ceramic target at substrate temperatures of 200, 300, 400, 500, and 600 °C. The deposition chamber was initially evacuated using a turbomolecular pump to a pressure in the range from 10⁻⁵ to 10⁻⁶ Torr and then filled with 99.99% pure oxygen at 350 mTorr. A pulsed Nd:YAG (yttrium aluminum garnet) laser was operated at a wavelength of 355 nm. The Zn_{1-x}Mg_xO thin films deposited at substrate temperatures of 200, 400, and 600 °C were annealed at 800 °C in a vacuum for 1 h. The Mg contents and thickness of the Zn_{1-x}Mg_xO thin films were measured using a Rutherford backscattering spectrometry (RBS). The thickness of the Zn_{1-x}Mg_xO thin films was measured to be approximately 1100–1350 nm. The crystalline quality was investigated by XRD with a Ni-filtered Cu K α ($\lambda = 1.5418 \times 10^{-10}$ m) source. The optical properties of the ZnO thin films were characterized by a PL with a 325 nm HeCd laser having a power of 20 mW as an excitation light source. The surface morphology was observed by an atomic force microscopy (AFM). The electrical properties were measured using Van der Pauw-Hall measurements. All measurements were performed at room temperature.

III. RESULTS AND DISCUSSION

Figure 1 shows the typical RBS spectra of the Zn_{1-x}Mg_xO thin films deposited at 200–600 °C. Figure 2 is a plot of the Mg/Zn ratio of Zn_{1-x}Mg_xO thin films as a function of the deposition temperature. The ratio of Mg/Zn clearly increased from 0.13 to 0.26 with the increasing substrate temperature from 200 to 600 °C because the Zn-related species can be desorbed more easily than Mg at high growth temperatures.

^{a)}Electronic mail: sylee@yonsei.ac.kr

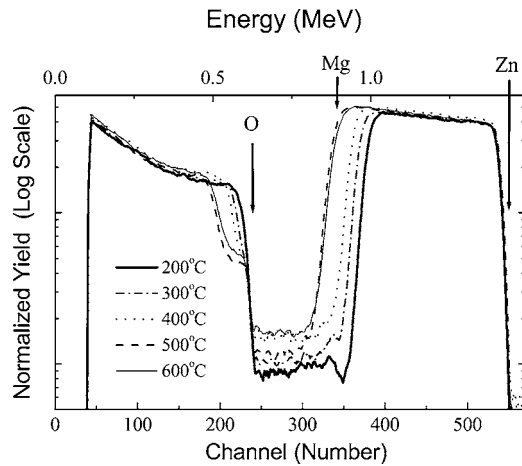


FIG. 1. Typical RBS spectra of $\text{Zn}_{1-x}\text{Mg}_x\text{O}$ thin films deposited at substrate temperatures of 200–600 °C.

The PL spectra of $\text{Zn}_{1-x}\text{Mg}_x\text{O}$ thin films deposited at substrate temperatures of 200 to 600 °C have been measured, as shown in Fig. 3. It was found that the ultraviolet (UV) peak position of the pure ZnO thin films deposited on (001) sapphire substrates were approximately 3.26 eV (380 nm), as has been reported previously.⁹ As the substrate temperature increases, the peak UV position of the $\text{Zn}_{1-x}\text{Mg}_x\text{O}$ thin films in Fig. 3 shows a blueshift indicating a band gap expansion. The optical band gap of $\text{Zn}_{1-x}\text{Mg}_x\text{O}$ thin films measured by PL expanded from 3.351 eV (370 nm) to 3.483 eV (356 nm) as the substrate temperature increased. Thus, it could be suggested that the increase of the optical band gap energy results from the increase in the Mg composition in the $\text{Zn}_{1-x}\text{Mg}_x\text{O}$ thin films. The strongest UV intensity was observed in the $\text{Zn}_{1-x}\text{Mg}_x\text{O}$ thin film deposited at the substrate temperature of 400 °C. This is consistent with the PL results of the pure ZnO thin films from our earlier work.¹⁰ The intensity of the UV emission of the ZnO thin film is dependent on the microcrystalline structure and stoichiometry.^{11,12} The melting points of Zn and Mg are 693 and 922 K, respectively.¹³ Above the substrate temperature of 400 °C, the Zn evaporation in $\text{Zn}_{1-x}\text{Mg}_x\text{O}$ thin films occurs and consequently results in the degradation of the stoichiometry of $\text{Zn}_{1-x}\text{Mg}_x\text{O}$ thin films.

Figure 4 shows the XRD spectra of the $\text{Zn}_{1-x}\text{Mg}_x\text{O}$ thin

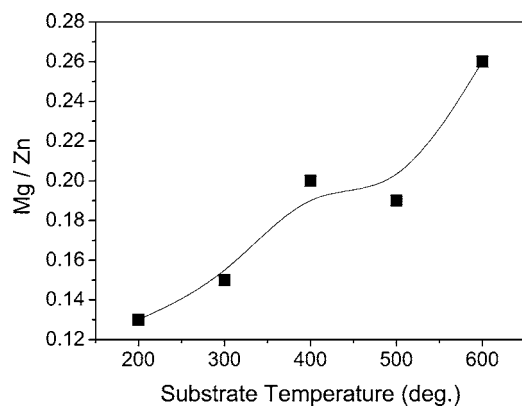


FIG. 2. The Mg/Zn ratio of $\text{Zn}_{1-x}\text{Mg}_x\text{O}$ thin films deposited at substrate temperatures of 200–600 °C.

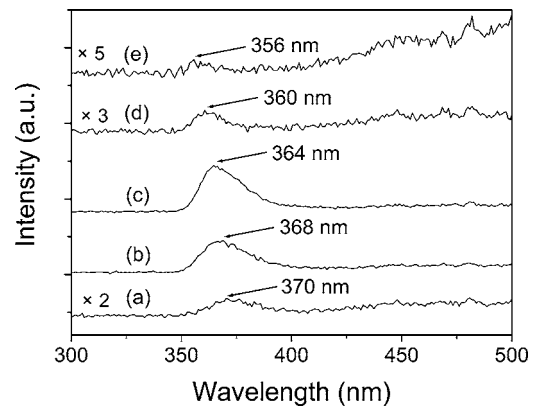


FIG. 3. PL spectra of $\text{Zn}_{1-x}\text{Mg}_x\text{O}$ thin films deposited at substrate temperatures of (a) 200, (b) 300, (c) 400, (d) 500, and (e) 600 °C.

films deposited at various substrate temperatures. All $\text{Zn}_{1-x}\text{Mg}_x\text{O}$ thin films were found to be *c* axis oriented and all exhibited a single phase of ZnO hexagonal structure without a cubic MgO structure. The $\text{Zn}_{1-x}\text{Mg}_x\text{O}$ thin films deposited at substrate temperatures of 200 to 600 °C show dominant (002), minor (100), and XRD (101) peaks. However, the (100) and (101) peaks of the $\text{Zn}_{1-x}\text{Mg}_x\text{O}$ thin film deposited at a substrate temperature of 200 °C were observed significantly. It is considered that the decrease of the adatom mobility of the species arriving on the substrate at a relatively low deposition temperature leads to the increase of the (100) and (101) peaks.

The full widths at half maximums (FWHMs) of the (002) peaks of the $\text{Zn}_{1-x}\text{Mg}_x\text{O}$ thin films and pure ZnO thin films depending on substrate temperatures are exhibited in Fig. 5. The FWHMs of all $\text{Zn}_{1-x}\text{Mg}_x\text{O}$ thin films were larger than that of the pure ZnO thin films deposited with the same conditions due to the strain in the film induced by the Mg alloy.³ The FWHMs decreased as the substrate temperature increased until 500 °C. This indicates the improvement of the crystalline quality of the thin films.¹⁴ The improvement of the crystalline quality of the thin films is mainly due to the increase of the adatom mobility of the atomic and molecular species on the substrate with the increasing substrate temperature. While the FWHMs of the pure ZnO thin films decreased due to sufficient adatom mobility as the substrate temperature increased, the FWHMs of the $\text{Zn}_{1-x}\text{Mg}_x\text{O}$ thin

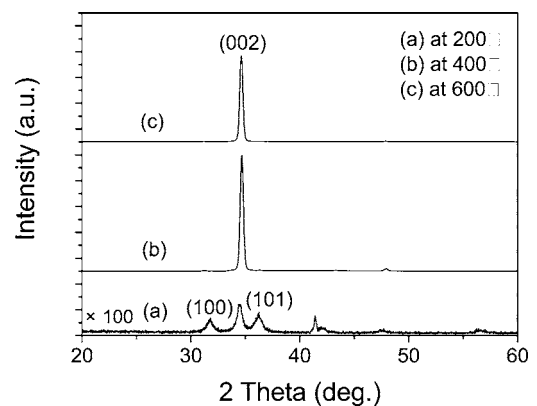


FIG. 4. XRD spectra of $\text{Zn}_{1-x}\text{Mg}_x\text{O}$ thin films deposited at substrate temperatures of (a) 200, (b) 400, and (c) 600 °C.

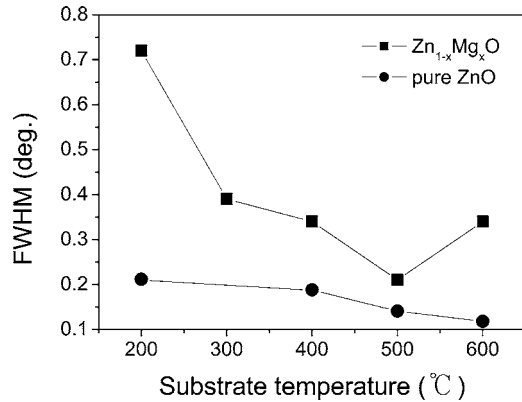


FIG. 5. Comparison of FWHMs of the (002) peak of the $Zn_{1-x}Mg_xO$ thin films and pure ZnO thin films deposited at substrate temperatures of 200–600 °C.

films grown above 500 °C increased despite sufficient adatom mobility on the substrate. This result indicates that the increase of the Mg composition in the $Zn_{1-x}Mg_xO$ thin film could lead to more strain in the film.³

The AFM images of the $Zn_{1-x}Mg_xO$ thin films deposited at substrate temperatures of 200, 400, and 600 °C have been observed, as shown in Fig. 6. The rms roughness of the $Zn_{1-x}Mg_xO$ thin films increased due to larger grains being generated by the increased amount of adatom mobility as the substrate temperature increased. According to Scherrer's formula, the increase of the grain size in the film indicates the decrease of the FWHM of the XRD spectra.¹⁵ Though the largest grain size was observed in the $Zn_{1-x}Mg_xO$ thin film deposited at a substrate temperature of 600 °C, as shown in Fig. 6, the FWHM of the (002) peak in the $Zn_{1-x}Mg_xO$ thin film deposited at 600 °C was the same as that of the $Zn_{1-x}Mg_xO$ thin film deposited at the substrate temperature of 400 °C, as shown in Fig. 5. The $Zn_{1-x}Mg_xO$ thin film deposited at the substrate temperature of 600 °C had more strain than the $Zn_{1-x}Mg_xO$ thin film deposited at 400 °C due to a higher Mg composition. Therefore, the FWHM of the (002) peak in the $Zn_{1-x}Mg_xO$ thin film deposited at 600 °C was the same as that of the $Zn_{1-x}Mg_xO$ thin film deposited at 400 °C despite the larger grain size.

Ideally, a defect-free ZnO film is an insulator; however, the as-grown films show *n*-type semiconducting properties with many defects, such as oxygen vacancies and Zn interstitials. Figure 7 shows the electron concentration and resistivity of the $Zn_{1-x}Mg_xO$ thin films and pure ZnO thin films deposited at substrate temperatures of 200, 400, and 600 °C. All $Zn_{1-x}Mg_xO$ and pure ZnO thin films have been *n*-type semiconductors and the resistivity was inversely proportional to the carrier concentration. The $Zn_{1-x}Mg_xO$ thin film deposited at a substrate temperature of 200 °C shows a higher resistivity than those deposited at 400 and 600 °C. Due to the low-temperature deposition, this film has a poor structure as shown in the XRD data in Figs. 4 and 5. The large resistivity was due to structural defects such as dislocations, dangling bonds, and trap centers in many grain boundaries. The resistivity of the $Zn_{1-x}Mg_xO$ thin film deposited at a substrate temperature of 400 °C decreased remarkably. This result was the outcome of the recovery of the structural defects

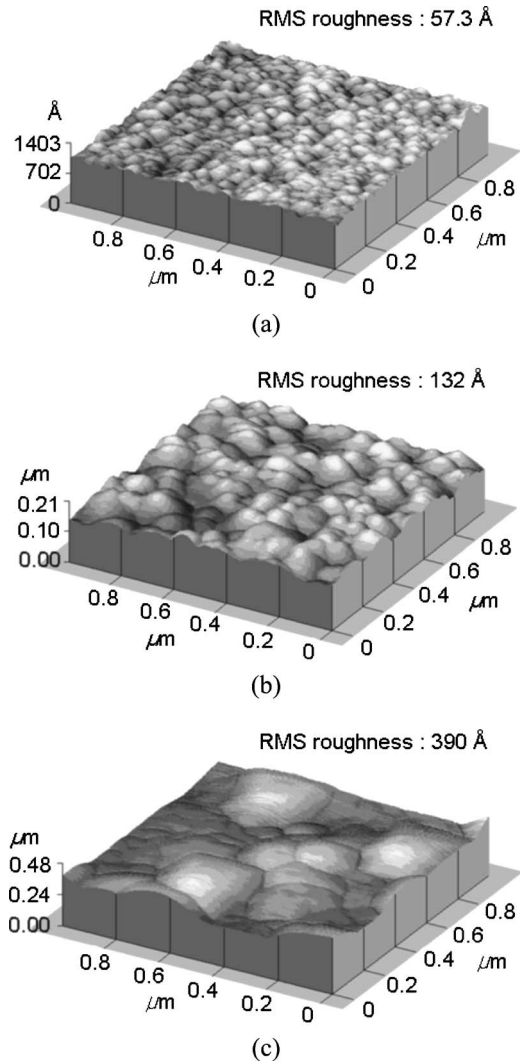


FIG. 6. AFM images of the $Zn_{1-x}Mg_xO$ thin films deposited at substrate temperatures of (a) 200, (b) 400, and (c) 600 °C.

by supplying enough thermal energy. However, the resistivity of the $Zn_{1-x}Mg_xO$ thin film deposited at a higher substrate temperature of 600 °C increased.

As mentioned before, Zn-related species are easily desorbed at higher growth temperatures and Zn evaporation occurs at substrate temperatures over 400 °C because the melting point of Zn is 419 °C. Therefore, many Zn vacancies might exist in the $Zn_{1-x}Mg_xO$ thin film deposited at 600 °C. It has been reported that the Zn vacancy acted as a dominant acceptor in an *n*-type ZnO film.^{16,17} The increase of Zn vacancies in the *n*-type $Zn_{1-x}Mg_xO$ thin film deposited at 600 °C could reduce electron concentration and increase resistivity. These tendencies are observed in the case of the pure ZnO film shown in Fig. 7(b). However, there are several differences between the pure ZnO and $Zn_{1-x}Mg_xO$ films. The electron concentration of the pure ZnO film is higher than that of the $Zn_{1-x}Mg_xO$ film, as shown in Figs. 7(a) and 7(b). The XRD result shown in Fig. 5 indicates that the film quality of ZnO films is better than that of the $Zn_{1-x}Mg_xO$ thin films. Consequently, the Mg in the ZnO film plays a role in degrading the film quality and decreasing the electron concentration compared with pure ZnO films. Also, as the sub-

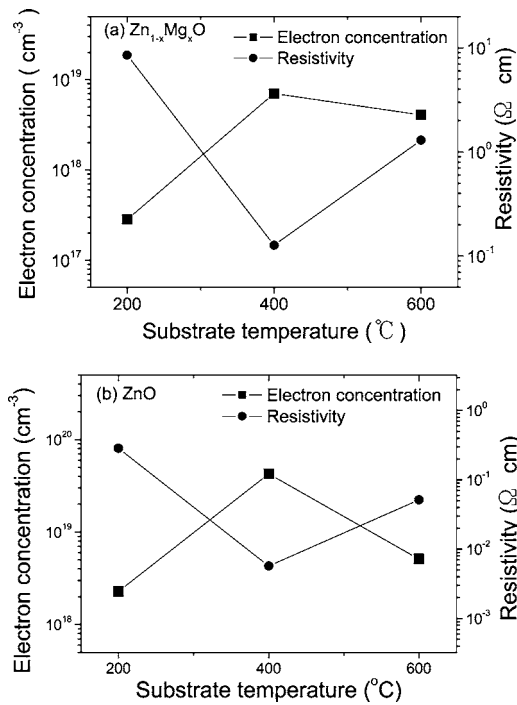


FIG. 7. The electron concentration and resistivity of (a) $Zn_{1-x}Mg_xO$ thin films and (b) pure ZnO thin films deposited at substrate temperatures of 200, 400, and 600 $^{\circ}C$.

strate temperature increases from 400 to 600 $^{\circ}C$, the resistivity of ZnO increased linearly according to the decrease of the carrier concentration, as shown in Fig. 7(b). However, this linearly inverse dependence of $Zn_{1-x}Mg_xO$ at deposition temperatures of 400–600 $^{\circ}C$ is different from the results of the pure ZnO shown in Fig. 7(b). The electron concentration of $Zn_{1-x}Mg_xO$ decreases by less than a factor of 2, approximately, while the resistivity increases by one order of magnitude, as shown in Fig. 7(a). This is in contrast to the decrease in the carrier concentration of ZnO between 400 and 600 $^{\circ}C$, which is accompanied by a corresponding increase in the resistivity, as shown in Fig. 7(b). The reason for the nonlinear inverse behavior between the electron concentration and resistivity of $Zn_{1-x}Mg_xO$ could be explained from the results of Figs. 3, 5, and 6. Figure 6 shows that the $Zn_{1-x}Mg_xO$ thin film deposited at 600 $^{\circ}C$ has the largest grain size. However, the grain size analysis from Scherrer's formula using the FWHMs of XRD, as shown in Fig. 5, reveals that the grain size of $Zn_{1-x}Mg_xO$ thin film fabricated at 400 $^{\circ}C$ is almost equal to those of the films fabricated at 600 $^{\circ}C$. As mentioned before, it is because the $Zn_{1-x}Mg_xO$ thin film deposited at a substrate temperature of 600 $^{\circ}C$ has more strain than the $Zn_{1-x}Mg_xO$ thin film deposited at 400 $^{\circ}C$ due to a higher Mg composition. Such strain in $Zn_{1-x}Mg_xO$ causes the results of the FWHMs, which are not proportional to the grain size measured by the AFM measurement (Fig. 6), as well as the optical properties degradation (Fig. 3). Therefore, the ratio of resistivity increases and electron concentration decreases of $Zn_{1-x}Mg_xO$ thin films, as shown in Fig. 7(a), are not the same as the results of the pure ZnO film shown in Fig. 7(b).

The PL peak positions of the $Zn_{1-x}Mg_xO$ thin films deposited at 200 and 400 $^{\circ}C$ were shifted to a shorter wave-

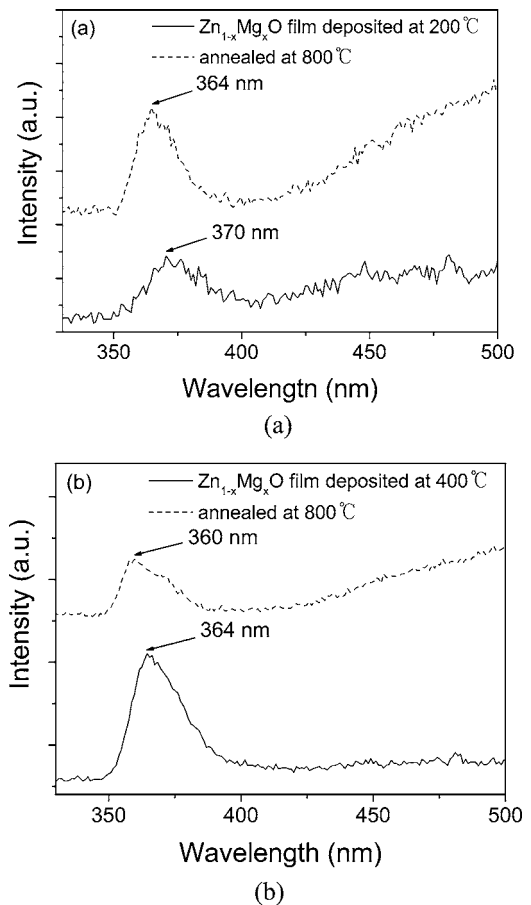


FIG. 8. PL spectra of $Zn_{1-x}Mg_xO$ thin films deposited at substrate temperatures of (a) 200 and (b) 400 $^{\circ}C$ with the PL spectra of post annealed $Zn_{1-x}Mg_xO$ thin films at 800 $^{\circ}C$.

length by 6 nm (from 370 to 364 nm) and 4 nm (from 364 to 360 nm), respectively, after postannealing at 800 $^{\circ}C$ as shown in Fig. 8. The $Zn_{1-x}Mg_xO$ thin films deposited at a low temperature did not have sufficient energy to bond, so these films would have unstable bonds with many defects. The preferential desorption of Zn atoms, due to their higher vapor pressure among the species in unstable bonding states and the substitution of interstitial Mg atoms into Zn vacancies, could result in the increase of the Mg composition in the $Zn_{1-x}Mg_xO$ thin films. Therefore, the PL peak position of the $Zn_{1-x}Mg_xO$ thin film deposited at a substrate temperature of 200 $^{\circ}C$ exhibited a greater shift than that of the $Zn_{1-x}Mg_xO$ thin film deposited at a substrate temperature of 400 $^{\circ}C$.

The $Zn_{1-x}Mg_xO$ thin films deposited at substrate temperatures of 200, 400, and 600 $^{\circ}C$ were annealed at 800 $^{\circ}C$ in a vacuum. The electron concentration and resistivity of these thin films are shown in Fig. 9. The increase of the electron concentration and the decrease of resistivity were observed in all thin films.

When a ZnO thin film is heated at high temperatures, it tends to lose oxygen.^{18,19} The increase of the electron concentration after postannealing at 800 $^{\circ}C$ was attributed to the generation of many defects by the reevaporation of oxygen at a high temperature. The reaction expressions are as follows:



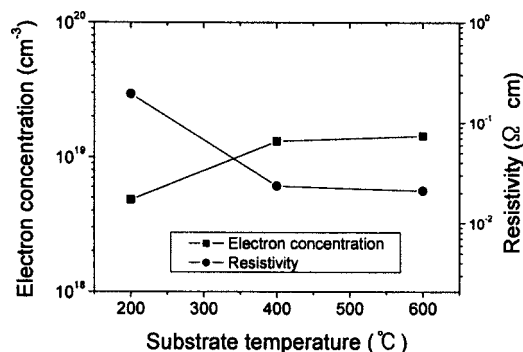
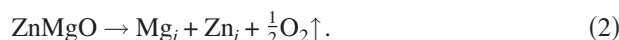


FIG. 9. The electron concentration and resistivity of $\text{Zn}_{1-x}\text{Mg}_x\text{O}$ thin films annealed at 800 °C in a vacuum. The $\text{Zn}_{1-x}\text{Mg}_x\text{O}$ thin films were deposited at substrate temperatures of 200, 400, and 600 °C.



As a result, oxygen vacancies and Zn and Mg interstitials are generated; these act as donors in $\text{Zn}_{1-x}\text{Mg}_x\text{O}$ thin films. Therefore, the electron concentration increases and the resistivity decreases. Furthermore, since postannealing was performed in a vacuum, not in ambient oxygen, the reevaporation of oxygen could occur more easily.

IV. CONCLUSION

$\text{Zn}_{1-x}\text{Mg}_x\text{O}$ thin films were deposited by pulsed laser deposition at various substrate temperatures using a ZnMgO ceramic target. The optical bandgap of $\text{Zn}_{1-x}\text{Mg}_x\text{O}$ thin films expanded due to the increase of the Mg composition in the $\text{Zn}_{1-x}\text{Mg}_x\text{O}$ thin films as the substrate temperature increased. The most intense UV emission was observed in the $\text{Zn}_{1-x}\text{Mg}_x\text{O}$ thin film deposited at a substrate temperature of 400 °C due to the Zn evaporation in $\text{Zn}_{1-x}\text{Mg}_x\text{O}$ thin films grown above 400 °C. According to the XRD results, all thin films exhibited good *c* axis orientation and the $\text{Zn}_{1-x}\text{Mg}_x\text{O}$ thin film deposited at a substrate temperature of 500 °C showed the best crystalline quality. The grain size and rms roughness of the $\text{Zn}_{1-x}\text{Mg}_x\text{O}$ thin films increased as the substrate temperature increased and the electron concentration and resistivity of the $\text{Zn}_{1-x}\text{Mg}_x\text{O}$ thin films varied with the

substrate temperature. The expansion of the optical band gap in $\text{Zn}_{1-x}\text{Mg}_x\text{O}$ thin films deposited at low temperatures of 200 and 400 °C was observed after postannealing at 800 °C. The electron concentration increased and the resistivity decreased after postannealing at 800 °C. These results indicate that the properties of $\text{Zn}_{1-x}\text{Mg}_x\text{O}$ thin films depend remarkably on substrate temperatures and the postannealing treatment with changes in the Mg composition.

ACKNOWLEDGMENT

This work was supported by Grant No. R01-2004-000-10195-0 (2005) from the Basic Research Program of the Korea Science and Engineering Foundation.

- ¹Y. Chen, D. Bagnall, and T. Yao, *Mater. Sci. Eng., B* **75**, 190 (2000).
- ²T. Makino *et al.*, *Appl. Phys. Lett.* **78**, 1979 (2001).
- ³W. I. Park, G.-C. Yi, and H. M. Jang, *Appl. Phys. Lett.* **79**, 2022 (2001).
- ⁴G. Venkata Rao, F. Säuberlich, and A. Klein, *Appl. Phys. Lett.* **87**, 032101 (2005).
- ⁵D. Zhao, Y. Liu, D. Shen, Y. Lu, J. Zhang, and X. Fan, *J. Appl. Phys.* **90**, 5561 (2001).
- ⁶A. Ohtomo, M. Kawasaki, T. Koida, K. Masubuchi, and H. Koinuma, *Appl. Phys. Lett.* **72**, 2466 (1998).
- ⁷S. Choojun, R. D. Vispute, W. Yang, R. P. Sharma, and T. Venkatesan, *Appl. Phys. Lett.* **80**, 1529 (2002).
- ⁸J. S. Kang, H. S. Kang, S. S. Pang, E. S. Shim, and S. Y. Lee, *Thin Solid Films* **443**, 5 (2003).
- ⁹H. S. Kang, J. S. Kang, J. W. Kim, and S. Y. Lee, *J. Appl. Phys.* **95**, 1246 (2004).
- ¹⁰S. H. Bae, S. Y. Lee, B. J. Jin, and S. Im, *Appl. Surf. Sci.* **169–170**, 525 (2001).
- ¹¹Z. K. Tang, Q. K. L. Wong, and P. Yu, *Appl. Phys. Lett.* **72**, 3270 (1998).
- ¹²B. J. Jin, S. H. Bae, S. Y. Lee, and S. Im, *Mater. Sci. Eng., B* **71**, 301 (2000).
- ¹³C. Kittel, *Introduction to Solid State Physics*, 7th ed. (Wiley, New York, 1996), p. 58.
- ¹⁴J. Zhenguo, L. Kun, Y. Chengxing, F. Ruixin, and Y. Zhizhen, *J. Cryst. Growth* **253**, 246 (2003).
- ¹⁵B. D. Cullity and S. R. Stock, *Elements of X-ray Diffraction*, 3rd. ed. (Prentice-Hall, Englewood Cliffs, NJ, 2001), p. 170.
- ¹⁶F. Tuomisto, V. Ranki, and K. Saarinen, *Phys. Rev. Lett.* **91**, 205502 (2003).
- ¹⁷A. F. Kohan, G. Ceder, and D. Morgan, *Phys. Rev. B* **61**, 15019 (2000).
- ¹⁸L. V. Azaroff, *Introduction to Solids* (McGraw-Hill, New York, 1960), p. 371.
- ¹⁹K. Ogata, K. Sakurai, Sz. Fujita, Sg. Fujita, and K. Matsushige, *J. Cryst. Growth* **214/215**, 312 (2000).